EARTHQUAKE ENGINEERING AND STRUCTURAL DYNAMICS, VOL. 25, 1405–1420 (1996)

SEQUENTIAL STIFFNESS DESIGN FOR SEISMIC DRIFT RANGES OF A SHEAR BUILDING–PILE–SOIL SYSTEM

TSUNEYOSHI NAKAMURA, IZURU TAKEWAKI
Department of Architectural Engineering, Kyoto University, Sakyo-ku, Kyoto 606, Japan

AND

YASUHIKO ASAOKA
Obayashi Corporation, Bunkyo-ku, Tokyo 113, Japan

SUMMARY

A shear building supported by a prescribed pile–soil system is subjected to bedrock earthquake input. A new design procedure is presented for generating a sequence of stiffness designs satisfying the constraints on interstorey drifts. The mean peak interstorey drifts of the shear building subjected to a set of spectrum-compatible ground motions at the bedrock are evaluated by a modal combination rule. Tuning of the fundamental natural period of a shear building with a fixed base with that of a shear beam ground results in a non-monotonic sequence of stiffness designs with respect to a ground stiffness parameter and previous approaches cannot be applied to such a problem. This difficulty in finding such a non-monotonic sequence is overcome by utilizing the ground stiffness parameter and the superstructure stiffness parameter alternately in multiple design phases and by developing a new multi-phase perturbation technique. Fundamental characteristics of this sequence of stiffness designs and the effect of ground stiffnesses on the design of the shear building are disclosed. It is further shown that the stiffness contour method is also useful for the design procedure such that a scattering effect in the estimates of ground stiffnesses is taken into account. The usefulness of the proposed procedure of sequential stiffness design and contour line method is demonstrated through several sequential design examples.

KEY WORDS: hybrid inverse problem; stiffness design; sequence of stiffness designs; building–pile–soil system; seismic drift constraint

1. INTRODUCTION

The problem considered in this paper is to find a set of stiffnesses of a building model which would exhibit a specified set of mean maximum response drifts under a set of design moderate earthquakes defined at bedrock with respect to a specified design spectrum. The building model here is to be supported by a simplified pile–soil interactive system as shown in Figure 1.[1–3] Such a design problem is in essence an inverse problem to a problem of seismic response analysis in the sense that the element properties of a building such as storey stiffnesses are to be found while the seismic response quantities such as drifts are to take on the prescribed values. It appears that, while much work has been conducted for disclosing the response characteristics of a building–pile–soil system, only a few papers have been published for directly finding stiffnesses of a building structure which exhibits a specified desirable response under design-spectrum compatible earthquakes. While a researcher in the field of structure–pile–soil interactive system or a practical engineer may maintain that a more elaborate model[4–9] for seismic behavioural analysis would better serve for confirming that all the critical response quantities in a building model are within their prescribed limits, it should be noted that an analysis procedure can be started only after the element properties of the model have been *designed* tentatively. Some iterative improvement will be utilized so that all the behavioural inequalities would be satisfied.

The purpose of this paper is to present a more direct and systematic method of stiffness design of a building model supported by a pile–soil interactive system such that the mean maximum of the response drifts in

CCC 0098–8847/96/121405–16

Received 20 November 1995
Revised 18 July 1996

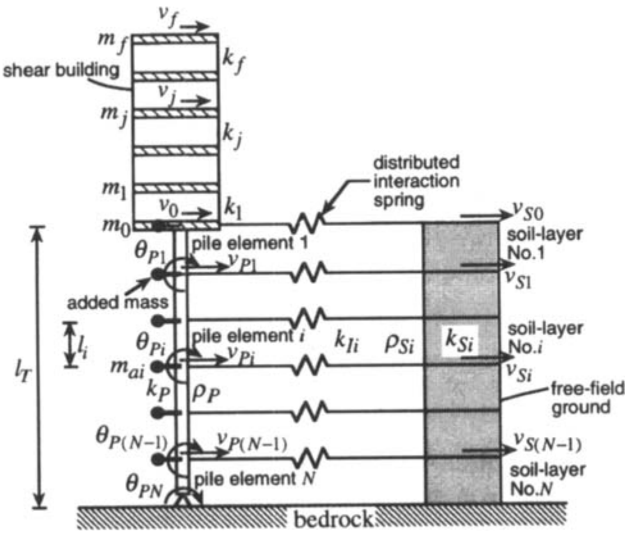

Figure 1. Simplified shear building–pile–soil system

every storey due to a set of design moderate earthquakes would coincide with a prescribed value. The basic idea of the new method is described here for a simplified building–pile–soil interactive system. Extension of the method towards those of a variety of elaborated models[4–9] for building-soil systems or building–pile–soil systems subjected to bedrock inputs may then be foreseen without much difficulty.

The senior authors have proposed a method of stiffness design such that the response drift distribution in a building supported by a pile–soil system subjected to design-spectrum compatible earthquakes would coincide with a specified distribution.[10] This design method, called the HIFDEM method, is a method combining the Hybrid Inverse Eigenmode Formulation[10,11] with a Design-Modification scheme[10,12] by regarding the fundamental natural period and the lowest mode as the principal parameters for adjustment. The stiffness design obtained from this design method will hereafter be called the Seismic response-Drift Constrained Stiffness design (SDCS design). In the previous paper,[10] it has been observed that, once the fundamental natural period of a shear building with a fixed base is tuned with that of a shear beam ground in such a system, as shown in Figure 1, with non-proportional damping, complicated characteristics as a primary–secondary system appear and it is difficult to apply the HIFDEM method to such a case. In this paper a new method for overcoming such a difficulty is proposed. The proposed method is based upon a new concept of a sequence of hybrid inverse problems and the corresponding sequence of SDCS designs with respect to a ground stiffness parameter. A series of stiffness designs can be found sequentially for a specified series of ground stiffness parameters. An initial design for the sequence of SDCS designs is obtained for a rather stiff ground for which the previous HIFDEM method can be effectively applied. Then a multi-phase perturbation method with respect to a ground stiffness parameter and a building stiffness parameter is devised.

The practical significance of this paper may be summarized as follows:

(1) A sequence of *hybrid* inverse problems is introduced and a sequence of SDCS designs with respect to a ground stiffness parameter not only discloses the effect of surface ground property on the design but also provides a designer with a range of candidate designs.
(2) A more elaborate model such as a finite element model may be desired for a building on a site with a complex topography. Once the backbone procedure is developed for a simplified model, then it provides a guideline for developing an efficient procedure for a practically acceptable model. In fact, the senior authors have already made an attempt to extend the HIFDEM method in this paper to that for a more realistic model consisting of a moment-resisting frame, a two-dimensional finite element

ground model and pile elements which satisfy deformation compatibility with the surrounding ground.[13]

(3) The equivalent soil stiffness may be estimated quite differently depending upon the level of shear strain in the soil and upon a method of testing. A set of several sequences of SDCS designs for different levels of specified response enables a designer to find a range of candidate designs in which the scattering effect in the estimates of soil stiffnesses has been taken into consideration.

(4) The proposed method of a sequence of stiffness designs has been developed only with respect to a set of design moderate earthquakes. The senior authors have however demonstrated that a 2-D- or 3-D-shear building model with a fixed base with the storey stiffnesses designed for specified mean maximum drifts well within the elastic limits under a set of design moderate earthquakes would exhibit a fairly similar inelastic mean peak drifts under a set of design major earthquakes with a similar spectral property.[12,14] In other words, the proposed method will provide a reliable lead towards a practically useful design procedure for a set of design major earthquakes.

2. SEQUENCE OF HYBRID INVERSE PROBLEMS AND SEQUENCE OF STIFFNESS DESIGNS

Consider a shear building–pile–soil system, shown in Figure 1, consisting of an f-storey shear building and a pile–soil system. The latter is represented by a pile, interaction springs and a shear beam ground model. Let $\mathbf{k}_S$ and $\mathbf{k}_F$ denote a vector of storey stiffnesses of the shear building and that of stiffnesses of the pile–soil system, respectively. The mean peak responses of the shear building–pile–soil system under a set of design-spectrum compatible earthquakes will be of main interest to the designer. In a usual design process, the objective of behavioural analysis is to find the mean peak interstorey drifts $\{\delta_{j\,\max}\}$ in the shear building with a specified set of stiffnesses $\bar{\mathbf{k}}_S$ and supported by the pile–soil system of stiffness $\bar{\mathbf{k}}_F$. Then $\delta_{j\,\max}$ may be expressed in terms of a response evaluation function F_j as follows:

$$\delta_{j\,\max} = F_j(\bar{\mathbf{k}}_S; \bar{\mathbf{k}}_F) \quad (j = 1, \dots, f) \tag{1}$$

F_j may be regarded as a mapping from $\bar{\mathbf{k}}_S$ and $\bar{\mathbf{k}}_F$ into $\delta_{j\,\max}$. In this paper the response spectrum method due to Yang *et al.*[15] is employed as the response evaluation method. The governing equations will be shown in the following section.

On the other hand, an inverse problem to behavioural analysis may be conceived. For a fixed-base shear building, a fully inverse problem can be posed such that all the storey stiffnesses are to be obtained for a specified set of mean peak interstorey drifts. For a shear building–pile–soil system, only a hybrid inverse problem[11] may be posed for the purpose of design due to the circumstance where the stiffnesses $\bar{\mathbf{k}}_F$ of the pile–soil system are prescribed. The objective of the hybrid inverse problem is to find $\mathbf{k}_S$ of the shear building, supported by the pile–soil system with $\bar{\mathbf{k}}_F$, such that every mean peak interstorey drift $\delta_{j\,\max}$ under a set of design-spectrum compatible earthquakes would be equal to $\bar{\delta}_j$. The response constraints in the hybrid inverse problem may be written as

$$\delta_{j\,\max} = F_j(\mathbf{k}_S; \bar{\mathbf{k}}_F) = \bar{\delta}_j \quad (j = 1, \dots, f) \tag{2}$$

or in a compact form as

$$\mathbf{F}(\mathbf{k}_S; \bar{\mathbf{k}}_F) = \bar{\boldsymbol{\delta}} \tag{3}$$

Equation (3) may formally be solved for $\mathbf{k}_S$ as $\mathbf{k}_S = \mathbf{F}^{-1}(\bar{\boldsymbol{\delta}}; \bar{\mathbf{k}}_F)$ where $\mathbf{F}^{-1}$ denotes the inverse mapping of $\mathbf{F}$ from $\bar{\boldsymbol{\delta}}$ to $\mathbf{k}_S$. Equation (3) is a set of complicated non-linear equations in terms of $\mathbf{k}_S$ and an elaborate computational scheme will usually be required to obtain $\mathbf{k}_S$. For a fixed-base shear building with a fundamental natural period close to that of the shear beam ground, the uniqueness of $\mathbf{k}_S$ satisfying equation (3) will no longer be guaranteed and a procedure for finding $\mathbf{k}_S$ from equation (3) will become much more complex. Furthermore, since the lowest-mode component of the overall system involving the shear beam ground with a fairly long fundamental natural period T_G will no longer be predominant, the HIFDEM method[10] due to the present authors cannot be applied to such a case.

In order to overcome this difficulty, a new concept referred to as a *sequence of hybrid inverse problems* is introduced here. Let ξ denote a parameter representing a sequence of stiffnesses of the ground and let $\bar{\mathbf{k}}_F(\xi)$ denote a specified sequence of stiffnesses of the pile–soil system in terms of ξ. Equation (3) written for one prescribed set $\bar{\mathbf{k}}_F$ and the corresponding solution $\mathbf{k}_S$ may then be extended so as to constitute a sequence of hybrid inverse problems as follows:

$$\mathbf{F}(\mathbf{k}_S(\xi); \bar{\mathbf{k}}_F(\xi)) = \bar{\boldsymbol{\delta}} \tag{4}$$

where the corresponding sequence of solutions is denoted by $\mathbf{k}_S(\xi)$. From equation (4) the *sequence* $\mathbf{k}_S(\xi)$ *of seismic response–drift constrained stiffness designs* (SDCS designs) may be formally written as

$$\mathbf{k}_S(\xi) = \mathbf{F}^{-1}(\bar{\boldsymbol{\delta}}; \bar{\mathbf{k}}_F(\xi)) \tag{5}$$

For a shear building–pile–soil system involving a shear beam ground model with a fairly large stiffness $\bar{\mathbf{k}}_F(0)$, the authors' method[10] may be applied due to its characteristics that the lowest-mode component is predominant in the estimate of the mean peak response and that tuning of the fundamental natural period of the shear building with a fixed base with that of the shear beam ground seldom occurs. The initial design is formally expressed as $\mathbf{k}_S(0) = \mathbf{F}^{-1}(\bar{\boldsymbol{\delta}}; \bar{\mathbf{k}}_F(0))$.

A sequence of SDCS designs of shear buildings each of which is supported by a pile–soil system with $\bar{\mathbf{k}}_F(\xi)$ close to $\bar{\mathbf{k}}_F(0)$ may be found by means of a Taylor series expansion of all the governing equations with respect to ξ about $\xi = 0$. Such a perturbation procedure breaks down as ξ approaches a limiting value such that some sensitivity coefficients with respect to ξ diverge. The purpose of the present paper is to develop a new multi-phase perturbation procedure for the regions of multiple SDCS designs with respect to ξ. A second perturbation parameter η is introduced for such a region and segments of the sequence of SDCS designs are successively found by means of piecewise series expansions.[16,17]

It is noted that in the usual numerical optimization procedure, design sensitivity coefficients of the response are computed with respect to the design variable vector $\mathbf{k}_S$ and an optimization procedure is applied to the search of just one optimum design. The procedure proposed here yields a sequence of SDCS designs described by piecewise series expansions with respect to a scalar parameter.

The design problem treated in this paper is described in Section 3 and the procedure for obtaining the initial design and the multi-phase perturbation method are presented in Sections 4 and 5. Design examples are shown in Section 6 and validity and accuracy of the present method are demonstrated in Section 7 by time-history response analysis.

3. STIFFNESS DESIGN PROBLEM FOR DESIGN EARTHQUAKES

In this paper a set of artificial ground motions compatible with a design velocity response spectrum is chosen as the design earthquakes. The design earthquakes are defined at bedrock. The design velocity response spectrum and the procedure of generating a set of design-spectrum compatible ground motions are shown in Appendix I. Figure 2 shows the compatibility of the mean velocity response spectrum of 20 generated ground motions for the damping ratio $h = 0{\cdot}02$ with the target velocity response spectrum These artificial ground motions are utilized only at the stage of accuracy verification of the present design method (Section 7). The design response spectrum alone is used in the design theory.

In order to describe the mapping F_j introduced in equation (1), the well-known complex eigenvalue analysis and the related response spectrum method[15] will be summarized briefly.

The Shear Building–Pile–Soil system in Figure 1 will be called an 'SBPS' model hereafter in this paper. Although the rotational degree of freedom of the base mat is neglected in this paper in order to present simply the essence of the design method, it is possible, if desired, to include its degree of freedom without difficulty. Furthermore, it is straightforward, if desired, to include the effect of group piles by introducing an appropriate procedure for evaluating the interaction spring coefficients.

Let f, N, N_T, N_{PG} denote the number of storeys of the shear building, the number of soil layers, the number of degrees of freedom of the overall system and the number of degrees of freedom of the pile–soil system. Let $\mathbf{M}, \mathbf{C}, \mathbf{K}$ denote the system mass, damping and stiffness matrices, respectively. These matrices of dimension

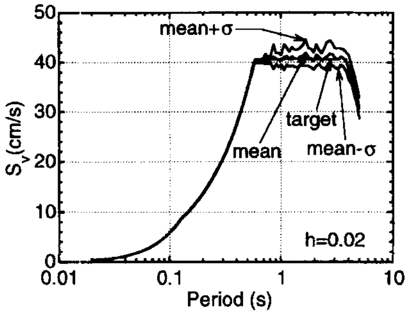

Figure 2. Design velocity response spectrum for damping ratio 0·02 defined at bedrock and mean spectrum of twenty artificial earthquakes generated by SIMQKE program

$N_T \times N_T$ may be expressed as

$$\mathbf{M} = \mathbf{M}_{PG} + \mathbf{M}_S, \qquad \mathbf{C} = \mathbf{C}_{PG} + \mathbf{C}_S, \qquad \mathbf{K} = \mathbf{K}_{PG} + \mathbf{K}_S \tag{6a–c}$$

where $\mathbf{M}_S, \mathbf{C}_S, \mathbf{K}_S$ denote the mass, damping and stiffness matrices of the shear building and $\mathbf{M}_{PG}, \mathbf{C}_{PG}, \mathbf{K}_{PG}$ denote those of the pile–soil system. $\mathbf{M}_S$ is the lumped mass matrix and $\mathbf{K}_S$ consists of the usual tridiagonal stiffness matrix. The damping matrix $\mathbf{C}_S$ is to be proportional to $\mathbf{K}_S$. The pile is divided into N elements according to the depths of the soil layers. In constructing the matrix $\mathbf{K}_{PG}$, only bending deformation of pile elements is considered with a cubic displacement function and only shear deformation is considered in the shear beam ground with a linear displacement function. The element stiffness matrix due to the interaction springs is shown in Appendix II. On the other hand, in constructing $\mathbf{M}_{PG}$, element consistent mass matrices of the pile elements and the shear beam ground are taken into consideration and added masses representing the inertial effect of soils around the pile are introduced as in References 5 and 10. $\mathbf{C}_{PG}$ can be constructed by superposing the damping matrices for each pile element, interaction springs in each soil layer and shear beam ground element in each soil layer. Under these assumptions, $\mathbf{C}$ may be expressed in terms of the element stiffness matrix $\mathbf{K}_l$ of dimension $N_T \times N_T$ for the lth subassemblage, the nominal damping ratio h_l for the lth subassemblage and the fundamental natural frequency $\omega^{(1)}$ of the overall system.

$$\mathbf{C} = \sum_l \frac{2h_l}{\omega^{(1)}} \mathbf{K}_l \tag{7}$$

The subassemblages consist of the shear building, each pile element, the interaction springs in each soil layer and the shear beam ground element in each soil layer.

Since this system has a non-proportional damping, complex eigenvalue analysis is required for accurate evaluation of seismic response. Let $\lambda^{(j)}$ and $\mathbf{u}^{(j)}$ denote the jth complex eigenvalue and the jth complex eigenvector of the overall system. Then the governing equation of the jth damped free vibration may be written as

$$(\lambda^{(j)2}\mathbf{M} + \lambda^{(j)}\mathbf{C} + \mathbf{K})\mathbf{u}^{(j)} = \mathbf{0} \tag{8}$$

Let $\lambda^{(j)}$ and $\mathbf{u}^{(j)}$ be expressed as

$$\lambda^{(j)} = \alpha^{(j)} + \beta^{(j)}\mathrm{i}, \qquad \mathbf{u}^{(j)} = \mathbf{\Phi}^{(j)} + \mathbf{\Psi}^{(j)}\mathrm{i} \tag{9a, b}$$

where i is the imaginary unit. The following normalization conditions are employed.

$$\mathbf{\Phi}^{(j)\mathrm{T}}\mathbf{M}\mathbf{\Phi}^{(j)} + \mathbf{\Psi}^{(j)\mathrm{T}}\mathbf{M}\mathbf{\Psi}^{(j)} = 1, \qquad \mathbf{\Phi}^{(j)\mathrm{T}}\mathbf{M}\mathbf{\Psi}^{(j)} = 0 \tag{10a, b}$$

The superscript T denotes the transpose of a vector. It should be noted that equation (10a) is equivalent to $\bar{\mathbf{u}}^{(j)\mathrm{T}}\mathbf{M}\mathbf{u}^{(j)} = 1$ ($\bar{\mathbf{u}}^{(j)}$ is the complex conjugate of $\mathbf{u}^{(j)}$) and equation (10b) is another normalization condition independent of equation (10a).

It is convenient to introduce the following complex participation factor for the jth eigenvibration (see, for example, Reference 18):

$$\nu^{(j)} = \frac{\mathbf{u}^{(j)^{\mathrm{T}}}\mathbf{M}\mathbf{1}}{\mathbf{u}^{(j)^{\mathrm{T}}}\mathbf{M}\mathbf{u}^{(j)}} \frac{1}{1 + (\varepsilon^{(j)} - \varepsilon_{\mathrm{d}}^{(j)})\mathrm{i}} = \nu_{\mathrm{R}}^{(j)} + \nu_{\mathrm{I}}^{(j)}\mathrm{i}, \tag{11}$$

where $\mathbf{1} = \{1 \cdots 1\}^{\mathrm{T}}$ and

$$\varepsilon^{(j)} = \frac{h^{(j)}}{\sqrt{1 - h^{(j)^2}}}, \qquad \varepsilon_{\mathrm{d}}^{(j)} = g_{\mathrm{R}}^{(j)} + g_{\mathrm{I}}^{(j)}\mathrm{i} \tag{12a, b}$$

$$g_{\mathrm{R}}^{(j)} + g_{\mathrm{I}}^{(j)}\mathrm{i} = \frac{1}{2\omega_{\mathrm{d}}^{(j)}} \frac{\mathbf{u}^{(j)^{\mathrm{T}}}\mathbf{C}\mathbf{u}^{(j)}}{\mathbf{u}^{(j)^{\mathrm{T}}}\mathbf{M}\mathbf{u}^{(j)}}, \qquad \omega_{\mathrm{d}}^{(j)} = \omega^{(j)}\sqrt{1 - h^{(j)^2}} \tag{12c, d}$$

The damping ratio $h^{(j)}$ and the natural frequency $\omega^{(j)}$ for the jth eigenvibration may be defined by

$$h^{(j)} = \bar{\mathbf{u}}^{(j)^{\mathrm{T}}}\mathbf{C}\mathbf{u}^{(j)}/(2\omega^{(j)}), \qquad \omega^{(j)^2} = \bar{\mathbf{u}}^{(j)^{\mathrm{T}}}\mathbf{K}\mathbf{u}^{(j)} \tag{13a, b}$$

The parameters $\alpha^{(j)}$ and $\beta^{(j)}$ in equation (9a) may be expressed as $\alpha^{(j)} = -\omega^{(j)}h^{(j)}$ and $\beta^{(j)} = \pm\,\omega^{(j)}\sqrt{1 - h^{(j)^2}}$ in terms of $h^{(j)}$ and $\omega^{(j)}$.

The mean peak interstorey drift in the kth storey may be evaluated by the response spectrum method due to Yang *et al.*[15]

$$\delta_{k\,\max} = \sqrt{\sum_{i=1}^{n}\sum_{j=1}^{n}\{\delta_{sk}^{(i)}\rho_{ss}^{(ij)}\delta_{sk}^{(j)} + 2\delta_{sk}^{(i)}\rho_{sc}^{(ij)}\delta_{ck}^{(j)} + \delta_{ck}^{(i)}\rho_{cc}^{(ij)}\delta_{ck}^{(j)}\}} \tag{14}$$

where n denotes the number of modes to be considered and $\delta_{sk}^{(i)}, \delta_{ck}^{(i)}, \rho_{ss}^{(ij)}, \rho_{cc}^{(ij)}, \rho_{sc}^{(ij)}$ are given by

$$\delta_{sk}^{(i)} = S_{\mathrm{Ds}}^{(i)}\,\mathrm{Re}\,[\nu^{(i)}\{u_k^{(i)} - u_{k-1}^{(i)}\}], \qquad \delta_{ck}^{(i)} = S_{\mathrm{Dc}}^{(i)}\,\mathrm{Im}\,[\nu^{(i)}\{u_k^{(i)} - u_{k-1}^{(i)}\}] \tag{15a, b}$$

$$\rho_{ss}^{(ij)} = 8a_{ij}c_{ij}\omega^{(i)}\omega^{(j)}/d_{ij}, \qquad \rho_{cc}^{(ij)} = \frac{4a_{ij}b_{ij}c_{ij}}{\{d_{ij}\sqrt{(1 + h^{(i)^2})(1 + h^{(j)^2})}\}} \tag{16a, b}$$

$$\rho_{sc}^{(ij)} = \frac{4a_{ij}\omega^{(i)}(b_{ij} - 2\omega_{\mathrm{d}}^{(j)^2})}{(d_{ij}\sqrt{1 + h^{(j)^2}})} \tag{16c}$$

The parameter $u_k^{(i)}$ denotes the component in $\mathbf{u}^{(i)}$ corresponding to the displacement of the kth lumped mass in the shear building. The parameters $a_{ij}, b_{ij}, c_{ij}, d_{ij}$ in equation (16) are shown in Appendix III. $S_{\mathrm{Ds}}^{(i)}$ is equivalent to the displacement response spectrum defined in equation (23) and $S_{\mathrm{Dc}}^{(i)}$ is assumed to be also equivalent to the latter. This assumption seems to be valid in the period range to be discussed here. Equation (14) completely defines mapping F_k introduced in equation (1).

Consider now a sequence of hybrid inverse problems described by equation (4) in Section 2. The stiffness vector $\bar{\mathbf{k}}_{\mathrm{F}}(\xi)$ may be evaluated on the basis of the shear moduli of soil layers. Consider N sequences of the shear moduli of N soil layers all of which are specified in terms of a parameter ξ $(0 \leqslant \xi \leqslant 1)$.

$$G_j(\xi) = (1 - \xi)G_{0j} + \xi G_{\mathrm{T}j} \quad (j = 1, \ldots, N) \tag{17}$$

Here G_{0j} denotes the shear modulus of the jth soil layer of a rather stiff ground for which an initial design $\mathbf{k}_{\mathrm{S}}(0) = \mathbf{F}^{-1}(\bar{\delta}; \bar{\mathbf{k}}_{\mathrm{F}}(0))$ defined in Section 2 is obtained without difficulty. $G_{\mathrm{T}j}$ denotes the terminal value of $G_j(\xi)$ which represents the shear modulus of a rather soft ground. The shear moduli $\{G_{\mathrm{T}j}\}$ are not necessarily proportional to $\{G_{0j}\}$. The interaction spring stiffness $k_{\mathrm{I}j}$ evaluated by the method[1,2] due to Penzien has a property to be proportional to the shear modulus of the jth soil layer. The problem for finding a Sequence $\mathbf{k}_{\mathrm{S}}(\xi)$ of Seismic response-Drift Constrained stiffness Designs as introduced in Section 2 may be stated as follows.

Problem SSDCD: Given a pile stiffness, ground shear moduli, i.e. equation (17), in terms of a parameter ξ, all the mass parameters, damping ratios in all subassemblages and a design velocity spectrum, find the sequence $\mathbf{k}_S(\xi) = \{k_1(\xi), \ldots, k_f(\xi)\}$ of SDCS designs of an SBPS model such that the mean peak interstorey drifts $\{\delta_{j\max}\}$ under the design-spectrum compatible earthquakes would coincide with the specified values $\{\bar{\delta}_j\}$.

In this paper the damping ratios of soil layers are treated to be constants independent of stiffnesses for a simpler presentation of the essential design procedure. For a realistic design, the shear moduli and the damping ratios of soil layers need to be evaluated according to the seismic strain levels. Once a relation of the damping ratio with the corresponding stiffness is determined through an analysis for the shear beam ground, it is straightforward to incorporate the relation into the present formulation.

4. SEQUENTIAL GENERATOR OF SDCS DESIGNS

4.1. *Initial design*

Problem SSDCD can be solved by finding an initial design $\mathbf{k}_S(0) = \mathbf{F}^{-1}(\bar{\boldsymbol{\delta}}; \bar{\mathbf{k}}_F(0))$ as described in Section 2 and by expanding $\mathbf{k}_S(\xi)$ with respect to ξ. An initial design problem for Problem SSDCD may be stated as follows.

Problem SSDCDI: Given a design velocity spectrum, a pile stiffness, a set $\{G_{0j}\}$ of ground shear moduli, all the mass parameters and damping ratios in all the subassemblages, find a set $\mathbf{k}_S(0) = \{k_1(0), \ldots, k_f(0)\}$ of superstructure storey stiffnesses of an SBPS model such that the mean peak interstorey drifts $\{\delta_{j\max}\}$ under the design-spectrum compatible earthquakes would coincide with the specified values $\{\bar{\delta}_j\}$.

An initial design can be efficiently obtained by the HIFDEM method stated before. Since the hybrid inverse eigenmode formulation[10,11] may be developed in terms of the undamped lowest eigenvector, the latter is utilized in this section only for obtaining the storey stiffnesses.

The procedure for solving Problem SSDCDI may be summarized as follows.

Step 1: Prescribe undamped lowest-mode interstorey-drift ratios $\{d_j/d_1\}$ so as to coincide with the specified mean peak interstorey-drift ratios $\{\bar{\delta}_j/\bar{\delta}_1\}$. Find the lowest eigenvalue Ω_1^0 of the SBPS model such that its mean peak interstorey drifts estimated only with the lowest-mode component would coincide with the specified values $\{\bar{\delta}_j\}$.

Step 2: Choose a small value $\Delta\Omega$. Find three sets of $\{k_j\}$ of the SBPS models which have the same lowest-mode interstorey drifts $\{d_j/d_1\} = \{\bar{\delta}_j/\bar{\delta}_1\}$ and three different lowest eigenvalues $\Omega_1^0 - \Delta\Omega$, Ω_1^0, $\Omega_1^0 + \Delta\Omega$ via the hybrid inverse eigenmode formulation.[10,11]

Step 3: Calculate the mean peak interstorey drifts of the three models obtained in Step 2 with the use of equation (14). Interpolate these three designs with a parabolic function in Ω_1–$\delta_{1\max}$ plane and find the lowest eigenvalue $\bar{\Omega}_1$ of the SBPS model such that $\delta_{1\max} \cong \bar{\delta}_1$ is satisfied.

Step 4: Find $\{k_j\}$ of that SBPS model which has the same lowest-mode interstorey drifts $\{d_j/d_1\} = \{\bar{\delta}_j/\bar{\delta}_1\}$ and the lowest eigenvalue $\bar{\Omega}_1$ via the hybrid inverse eigenmode formulation. Calculate $\{\delta_{j\max}\}$ of this model by equation (14).

Step 5: Update the lowest eigenmode by $d_j^{[m+1]} = (\bar{\delta}_j/\delta_{j\max})d_j^{[m]}$ until $\delta_{j\max}/\delta_{1\max} \cong \bar{\delta}_j/\bar{\delta}_1$ (for all j) are satisfied (m: cycle number).

Step 6: Stop if $|(\delta_{j\max}/\bar{\delta}_j) - 1| < \varepsilon$ (ε: small positive number) (for all j) are satisfied. Otherwise go to Step 2.

4.2. *Generator for a monotonic sequence of SDCS designs*

In Problem SSDCD all the design variables and field variables are regarded as functions of a parameter ξ. A variable regarded as a function of ξ is denoted by a hat $(\hat{\ })$ hereafter in this paper. Let us define the following vector $\hat{\mathbf{X}}$.

$$\hat{\mathbf{X}}^T = [\hat{\mathbf{x}}^{(1)^T}\ \hat{\mathbf{x}}^{(2)^T} \cdots \hat{\mathbf{x}}^{(n)^T}\ \hat{\mathbf{y}}^T\ \hat{\mathbf{z}}^{(11)^T}\ \hat{\mathbf{z}}^{(12)^T} \cdots \hat{\mathbf{z}}^{(n\,n-1)^T}\ \hat{\mathbf{z}}^{(nn)^T}] \tag{18}$$

where $\hat{\mathbf{x}}^{(i)}, \hat{\mathbf{y}}, \hat{\mathbf{z}}^{(ij)}$ denote the following vectors:

$$\hat{\mathbf{x}}^{(i)^{\mathrm{T}}} = \{\hat{\boldsymbol{\Phi}}^{(i)^{\mathrm{T}}}\hat{\boldsymbol{\Psi}}^{(i)^{\mathrm{T}}}\hat{\alpha}^{(i)}\hat{\beta}^{(i)}\hat{h}^{(i)}\hat{\omega}^{(i)}\hat{v}_{\mathrm{R}}^{(i)}\hat{v}_{\mathrm{I}}^{(i)}\hat{g}_{\mathrm{R}}^{(i)}\hat{g}_{\mathrm{I}}^{(i)}\hat{\varepsilon}^{(i)}\hat{S}_{\mathrm{Ds}}^{(i)}\hat{S}_{\mathrm{Dc}}^{(i)}\hat{\boldsymbol{\delta}}_s^{(i)^{\mathrm{T}}}\hat{\boldsymbol{\delta}}_c^{(i)^{\mathrm{T}}}\} \tag{19a}$$

$$\hat{\mathbf{y}}^{\mathrm{T}} = \{\hat{k}_1 \cdots \hat{k}_f \hat{\mathbf{c}}_g^{\mathrm{T}} \hat{c}_1 \cdots \hat{c}_f\}, \qquad \hat{\mathbf{z}}^{(ij)^{\mathrm{T}}} = \{\hat{\rho}_{ss}^{(ij)}\hat{\rho}_{cc}^{(ij)}\hat{\rho}_{sc}^{(ij)}\hat{a}_{ij}\hat{b}_{ij}\hat{c}_{ij}\hat{d}_{ij}\} \tag{19b, c}$$

In equation (19a) $\hat{\boldsymbol{\delta}}_s^{(i)} = \{\hat{\delta}_{sk}^{(i)}\}$ and $\hat{\boldsymbol{\delta}}_c^{(i)} = \{\hat{\delta}_{ck}^{(i)}\}$ where the elements have been defined in equations (15a, b) and $\hat{\mathbf{c}}_g$ in equation (19b) denotes a vector consisting of damping coefficients in pile–soil system.

For simple and exact expression, the vector $\hat{\mathbf{X}}$ consisting of functions of ξ is denoted by $\hat{\mathbf{X}}(\xi)$ hereafter. Now that $\hat{\mathbf{X}}(\xi_0)$ has been obtained as the solution to Problem SSDCDI, $\hat{\mathbf{X}}(\xi)$ may be expanded around $\xi = \xi_0$ as

$$\hat{\mathbf{X}}(\xi) = \hat{\mathbf{X}}(\xi_0) + (\xi - \xi_0)\hat{\mathbf{X}}'(\xi_0) + \tfrac{1}{2}(\xi - \xi_0)^2\hat{\mathbf{X}}''(\xi_0) + \cdots, \tag{20}$$

where $\hat{\mathbf{X}}'(\xi_0) = \mathrm{d}\hat{\mathbf{X}}(\xi)/\mathrm{d}\xi|_{\xi=\xi_0}$, etc. Substitution of equations (17) and (20) into equations (8) (into which equations (9a) and (9b) have been substituted), (10a, b), (11) (into which equation (12b) has been substituted), (12a), (12c), (13a, b), (14), (15a, b), (16a–c), (23), (7), (27a–d) and rearrangement with respect to each order of $(\xi - \xi_0)$ yield the following equations for determining $\hat{\mathbf{X}}'(\xi_0)$ and $\hat{\mathbf{X}}''(\xi_0)$.

$$\mathbf{A}\hat{\mathbf{X}}'(\xi_0) = \mathbf{b}_1 \tag{21}$$

$$\mathbf{A}\hat{\mathbf{X}}''(\xi_0) = \mathbf{b}_2 \tag{22}$$

where $\mathbf{A}$ is a coefficient square matrix of order $\{(11 + 7n + 2N_{\mathrm{T}})n + 2(n + 1)f + N_{\mathrm{PG}}\}$ and $\mathbf{b}_1, \mathbf{b}_2$ are known vectors including lower-order quantities. Equations (21) and (22) correspond to $\mathbf{F}'(\xi_0) = \mathbf{0}$ and $\mathbf{F}''(\xi_0) = \mathbf{0}$, respectively, in terms of mapping $\mathbf{F}$ defined in equation (4). Substitution of $\hat{\mathbf{X}}'(\xi_0)$ and $\hat{\mathbf{X}}''(\xi_0)$ obtained from equations (21) and (22) into equation (20) and application of the stepwise method[16,17] of Taylor series expansion enable one to compute $\hat{\mathbf{X}}(\xi)$ $(0 \leqslant \xi \leqslant 1)$. Second-order Taylor series expansion is recommended for better accuracy with a small number of steps.

4.3. Generator for a non-monotonic sequence of SDCS designs

Figure 3(a) shows an illustrative set of plots of natural periods of the overall system of SDCS designs in the later example with respect to fundamental natural period T_{G} of the shear beam ground and Figure 3(b) shows plots of storey stiffnesses of SDCS designs with respect to T_{G}. For simplicity the fundamental natural period of the shear beam ground is hereafter called the fundamental natural period of the ground. Since T_{G} has one-to-one correspondence with the parameter ξ introduced in equation (17), it is possible to interpret that expansion with respect to ξ is essentially equivalent to that with respect to T_{G}. It can be observed from Figures 3(a) and 3(b) that the generation procedure of SDCS designs with respect to T_{G} (or ξ) becomes divergent (e.g. $\mathrm{d}T_1/\mathrm{d}T_{\mathrm{G}} \to \infty$) in the neighbourhood of a state represented by say 'P1'. T_1 is the fundamental natural period of the overall system. The difficulty can be avoided by interchanging the expansion parameter T_{G} (or ξ) with the fundamental natural frequency $\omega^{(1)}(=2\pi/T_1)$ (or η in Section 2) of the overall system in an interval between a neighbourhood state of 'P1' and a neighbourhood state of 'P2'. The sequence of stiffness designs corresponding to the interval between the states 'P1' and 'P2' indicates the sequence $\hat{\mathbf{k}}_{\mathrm{S}}(\eta)$ stated in Section 2. The fundamental natural frequency $\omega^{(1)}$ of the overall system is almost equal to that of the shear building with a fixed-base in this region and can be regarded as a parameter for representing the stiffness of the shear building. It should be noted that $\hat{\omega}^{(1)}$ in the vector $\hat{\mathbf{x}}^{(1)}$ in equation (19a) must be replaced by the fundamental natural frequency $\omega_{\mathrm{G}}(=2\pi/T_{\mathrm{G}})$ of the ground as a new unknown variable and that the symbol $(\hat{\ })$ is regarded to indicate a function of $\omega^{(1)}$ instead of ξ. In this case the corresponding column in the coefficient matrix $\mathbf{A}$ in equations (21) and (22) and known constant vectors $\mathbf{b}_1$ and $\mathbf{b}_2$ must be modified. Beyond a neighbourhood state of 'P2' the expansion parameter is interchanged back to T_{G} (or ξ) and the sequence $\mathbf{k}_{\mathrm{S}}(\xi)$ can thereafter be sought sequentially.

It is apparent from Figures 3(a) and 3(b) that there exists a region of T_{G} for which three different designs and hence three T_1 values are possible. A question may arise as to which of the three designs is of practical significance. An answer to this question can be derived from a closer examination of the ground stiffness and sensitivity properties of the designs with respect to specified interstorey drifts. It should be noted that ground

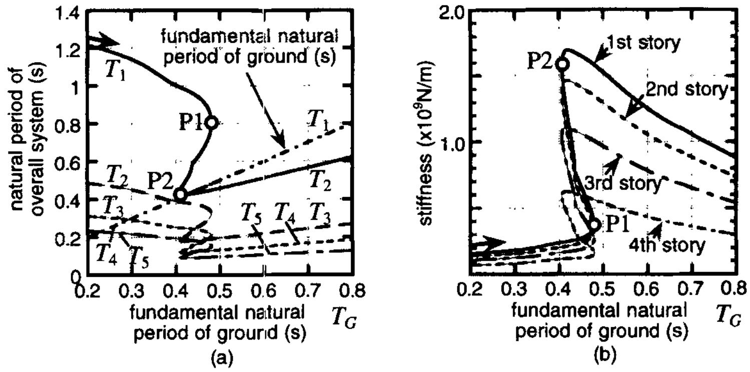

Figure 3. (a) Natural periods of overall systems of a sequence of seismic response-drift constrained stiffnesses designs with respect to fundamental natural period of ground; (b) Storey stiffnesses of shear building models of seismic response-drift constrained stiffness designs with respect to fundamental natural period of ground

stiffness values as estimated from the result of field tests involve almost always considerable errors. Any two different test procedures would yield two different mean value moduli depending upon the level of seismic strain which the layer of the ground experiences. A design concept will be presented in the following section for a series of ground stiffnesses representing their scattering effects. It should also be pointed out that greater response variations would correspond to smaller changes of ξ (or T_G) in the case where the middle set of storey stiffnesses is adopted and that the designs corresponding to the smallest and middle sets of storey stiffnesses disappear easily for smaller specification of interstorey drifts. These properties will be shown later in Figure 5. The largest set of storey stiffnesses may therefore be preferable in this region.

It should be noted that a design represented by a point in the region stated in the previous paragraph indicates the building model such that the fundamental period of the building with a fixed-base would be tuned with T_G and that designing a building in this region should be avoided, as far as possible. A theoretical examination into such a case may however be of some interest for laying the foundation of practical design regions.

It is also noted that the response amplification due to the tuning of the fundamental natural periods of the two systems may be less critical than indicated in Figure 3(b) because of non-linearities which could develop in the overall soil–pile–building system.

5. STIFFNESS CONTOUR METHOD FOR THE SCATTERING EFFECT IN ESTIMATES OF GROUND STIFFNESSES

The accuracy of the sequence of SDCS designs depends greatly on the accuracy of prediction of the dynamic behaviour of a pile–soil system adopted and hence on the accuracy of evaluation of the dynamic soil properties. If several different methods of evaluating shear and volumetric moduli of a set of soil layers were used, they would yield different estimates. The moduli depend also upon the strain levels that the soil layers experience. The mechanism of material damping in a soil–pile system is more complex and a hysteretic damping model may be more appropriate than a viscous damping model as adopted here. While the proposed theory may be extended to a system involving complex damping, a linear viscous damping model has been assumed here for simplicity of presentation.

In view of these factors of scattering, it seems more appropriate to regard the original problem for finding an SDCS design as that defined for a range or an interval $(\bar{G}_j - \Delta G_j, \bar{G}_j + \Delta G_j)$ of the shear moduli of the soil layers involved. $\bar{G}_j$ is the mean ground shear modulus in the jth soil layer and ΔG_j is half the interval of the estimated ground shear modulus. Since the overall stiffness of the ground may be represented by T_G, the corresponding interval of ground stiffness may be written as $(\bar{T}_G - \Delta T_{GL}, \bar{T}_G + \Delta T_{GU})$, where $\bar{T}_G$ corresponds

to $\{\bar{G}_j\}$ and $\bar{T}_G - \Delta T_{GL}$ and $\bar{T}_G + \Delta T_{GU}$ denote the lowest and highest values corresponding to $\bar{G}_j + \Delta G_j$ and $\bar{G}_j - \Delta G_j$, respectively. The problem of Seismic response-Drift Constrained Stiffness design subject to a set of Relaxed constraints is now considered:

Problem SDCSR: Given a pile stiffness, a set $\{\bar{G}_j - \Delta G_j \leqslant G_j \leqslant \bar{G}_j + \Delta G_j\}$ of intervals of ground shear moduli, all the mass parameters, damping ratios in all the subassemblages and a design velocity spectrum, find the SDCSR design $\tilde{\mathbf{k}}_S$ among a sequence $\mathbf{k}_S(\xi)$ of the SBPS model such that $\{\delta_{j\,\max}\}$ would be less than or equal to $\{\bar{\delta}_j\}$.

For this problem, it is convenient to define a set of contours of k_j as a function not only of T_G but also of multiplier ζ on the prescribed set $\{\bar{\delta}_j\}$. A set of proportional variations of the specified interstorey drifts $\{\bar{\delta}_j\}$ may first be defined by $\zeta\{\bar{\delta}_j\}$ where $1 - \mu \leqslant \zeta \leqslant 1 + \mu$ ($\mu = \Delta\delta/\bar{\delta}_j > 0$). For every ζ value, an SSDCD problem can be posed to find the sequence $\hat{\mathbf{k}}_S(T_G;\zeta)$. Hence a bundle of contours $\hat{k}_{Sj}(T_G;\zeta)$ may be drawn on a $(T_G, \hat{k}_{Sj})$-plane as illustrated in Figure 4. It is assumed here that a bundle of contours for $1 - \mu \leqslant \zeta \leqslant 1 + \mu$ forms a river of streamlines with neither intersection nor any void space of discontinuity as will be shown for an example in Figure 5. The solution to Problem SDCSR can then be obtained by embedding a line segment of length $\Delta T_{GL} + \Delta T_{GU}$ parallel to the T_G axis in each bundle so as to satisfy one of the following conditions:

(1) If $\partial\hat{k}_{Sj}(T_G;1)/\partial T_G < 0$, then $\tilde{k}_{Sj} = \hat{k}_{Sj}(\bar{T}_G - \Delta T_{GL};1)$ (region C).
(2) If $\partial\hat{k}_{Sj}(T_G;1)/\partial T_G > 0$, then $\tilde{k}_{Sj} = \hat{k}_{Sj}(\bar{T}_G + \Delta T_{GU};1)$ (region A).
(3) If $\partial\hat{k}_{Sj}(T_G;1)/\partial T_G = 0$ at $T_G = T_G^*$, then $\tilde{k}_{Sj} = \hat{k}_{Sj}(T_G^*;1)$ (region B).

Each solid circle in Figure 4 indicates the solution in each region.

It may be helpful to introduce the following interpretation in Figure 4. Let us pay attention to a point on a sequence of SDCS designs with the specified interstorey drifts $\{\bar{\delta}_j\}$ and draw a line segment through the point and parallel to T_G axis. Then variation of contour values along the line segment indicates the variation of mean peak interstorey drifts with respect to T_G keeping the storey stiffnesses of the shear building constant. It can be recognized from Figure 4 that, while, in region B discussed in Section 4.3, interstorey drifts become greater for variation of T_G toward a larger value in the case where the middle or smallest set of storey stiffnesses is adopted, those become smaller than $\{\bar{\delta}_j\}$ for any change of T_G in the case where the largest set of storey stiffnesses is adopted. For this reason, the largest set of storey stiffnesses has been chosen as the solution in the region B in Section 4.3.

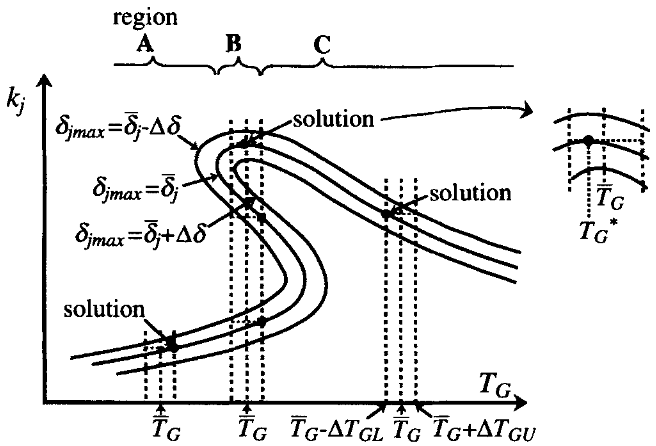

Figure 4. Schematic diagram of storey stiffnesses of shear building models of seismic response-drift constrained stiffness designs with respect to fundamental natural period of ground (three specified interstorey drifts)

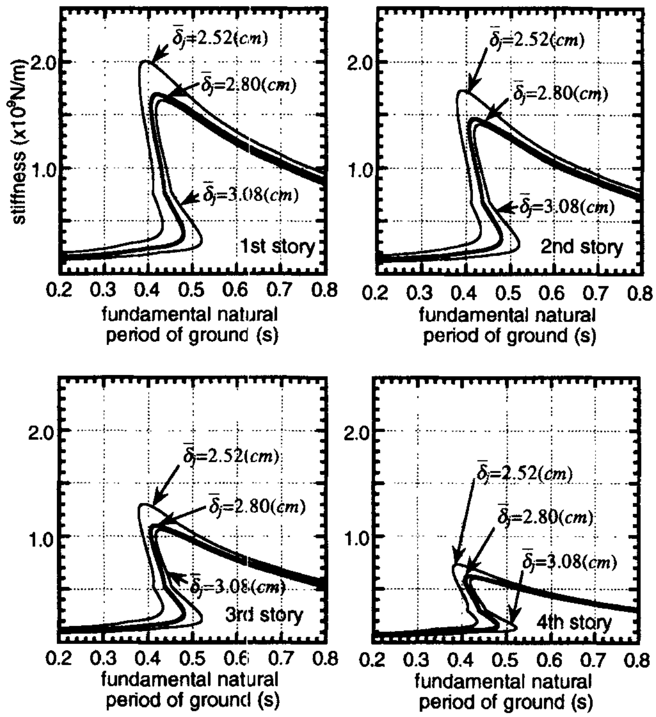

Figure 5. Storey stiffnesses of shear building models of seismic response-drift constrained stiffness designs with respect to the fundamental natural period of ground (three specified interstorey drifts)

6. DESIGN EXAMPLES

Consider an eight storey shear building and a shear beam ground of four soil layers. Each soil layer has the same thickness 4 m. The ground shear moduli $\{G_{Tj}\}$ and damping ratios have been obtained via the SHAKE program.[19] Those values are shown in Table I. The mass densities and interaction spring constants (Winkler spring coefficients) $\{k_{1i}\}$ of the soil layers are also shown in Table I. The interaction spring constants have been determined with the use of Mindlin's solution as in References 1 and 2. The ground shear moduli $\{G_{0j}\}$ for the initial design $\mathbf{k}_S(0)$ have been given by $20 \times \{G_{Tj}\}$. The area of shear beam ground has been chosen so that the mass of shear beam ground is about $1{\cdot}0 \times 10^6$ times the added mass in the same level and that any problem in numerical analysis due to large difference in the order of magnitude would not arise. The diameter of the pile is 1·5 m. The mass density and Young's modulus of concrete are 2300 kg/m^3 and $2{\cdot}06 \times 10^{10}$ N/m^2, respectively.

Each two storeys of the original 8-storey building is reduced to one lumped mass. The shear building has therefore four degrees of freedom. This model has been employed because tuning of the fundamental natural period of the shear building with a fixed base with that of the shear beam ground could occur in such a class of buildings. The lumped masses of the reduced shear building are $m_0 = 90 \times 10^3$ kg, $m_1 = \cdots = m_4 = 60 \times 10^3$ kg. The specified mean peak interstorey drifts are 2·8 cm which means the angle 1/250 rad of member rotation of a column for the original storey height 3·5 m (distance between masses in the reduced shear building model is 7 m). The damping ratios of the shear building and pile are 0·02 and 0·05, respectively. The damping ratios in Table I are for the soil layers. The number of eigenmodes in equation (14) is $n = 8$. The increment of ξ defined in equation (17) is $\Delta\xi = 0{\cdot}005$ and that of η is $\Delta\eta = 0{\cdot}005$.

Figure 3(a) shows plots of the first five natural periods (fundamental through the fifth) of the overall system of SDCS designs with respect to the fundamental natural period T_G of the ground. Figure 3(b) shows plots of

Table I. Shear moduli, damping ratios and interaction spring stiffnesses of layered soils

Soil layer no.	Density (kg/m^3)		Shear modulus ($\times 10^4$ N/m^2)	Damping ratio	Winkler spring coefficient ($\times 10^4$ N/m^2)
1	Clay	1680	769	0·048	2456
2	Sand	1800	632	0·099	1888
3	Sand	1800	812	0·106	2586
4	Silt	1900	966	0·107	3614

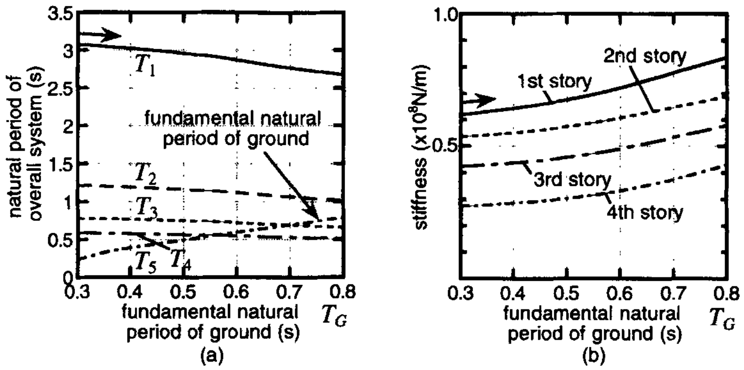

Figure 6. (a) Natural periods of overall systems of seismic response-drift constrained stiffness designs with respect to fundamental natural period of ground (tall building model); (b) Storey stiffnesses of shear building models of seismic response-drift constrained stiffness designs with respect to fundamental natural period of ground

storey stiffnesses of SDCS designs with respect to T_G. It can be observed from Figures 3(a) and 3(b) that the natural period and the sequence of SDCS designs have a similar non-monotonic property. As stated in Section 4.3, the expansion parameter has been changed from T_G (or ξ) to $\omega^{(1)}$ (or η) between the points 'P1' and 'P2'. It can be seen from Figure 3(b) that larger storey stiffnesses are required in the tuned region.

Figure 5 shows plots of three stiffness sequences of SDCS designs with respect to T_G for three different specified mean peak interstorey drifts 2.8, 2.8 ± 0.28 cm. It can be observed from Figure 5 that, if the middle set of storey stiffnesses is adopted in the region B shown in Figure 4, greater response variations correspond to smaller changes of T_G toward a longer period. It can also be seen from Figure 5 that the designs corresponding to the smallest and middle sets of storey stiffnesses in region B disappear easily for smaller specification of interstorey drifts, say 2.52 cm, and these designs have unstable characteristics. Preparation of a set of sequences of SDCS designs as shown in Figure 5 enables a designer to develop a design procedure in which a scattering effect in ground stiffness estimation explained in Section 5 is taken into consideration.

In order to show that a sequence of SDCS designs indicates a monotonic path in the model where the fundamental natural period of the shear building with a fixed base does not approach that of the ground, a sequence of SDCS designs has been obtained for the model where each five storeys of the original 20-storey building model are reduced to one lumped mass. The number of degrees of freedom of the shear building is still four. The specified mean peak interstorey drifts are 7.0 cm which correspond to the angle 1/250 rad of member rotation of columns. Figures 6(a) and 6(b) show plots of the natural periods (fundamental through the fifth) of the overall system of SDCS designs with respect to T_G and plots of storey stiffnesses of SDCS designs with respect to T_G, respectively. It can be seen from Figures 6(a) and 6(b) that the sequence of SDCS designs exhibits a monotonic behaviour for this model.

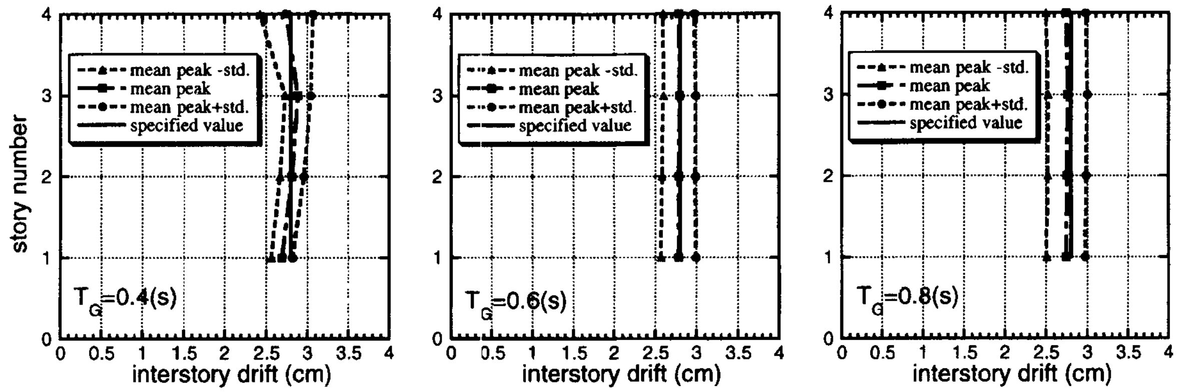

Figure 7. Distributions of mean peak values and mean peak $\pm\sigma$ values of interstorey drifts of seismic response-drift constrained stiffness designs subjected to twenty spectrum-compatible artificial earthquakes

7. VERIFICATION BY TIME-HISTORY RESPONSE ANALYSIS

In order to disclose the accuracy of this design method described in Sections 4.1–4.3 with a specific ground stiffness, time-history response analysis has been performed for a set of 20 spectrum-compatible bedrock motions described in Appendix I. The time-history response analysis has been performed in a matrix form using the non-proportional damping matrix defined in equation (7). Newmark-β method ($\beta = 0{\cdot}25$) has been utilized in the numerical integration. The time increment is 0·01 s.

Figure 7 shows the mean peak and mean peak $\pm\sigma$ distributions of the interstorey drifts in the three shear buildings designed for $T_G = 0{\cdot}4, 0{\cdot}6, 0{\cdot}8$ s. It can be observed from Figure 7 that the mean peak interstorey drifts computed coincide with the specified values within an accuracy of ± 5 per cent. It has also been assured that the mean peak interstorey drifts of the shear buildings (largest, middle and smallest sets of storey stiffnesses) designed in the region B shown in Figure 4 coincide with the specified values within an accuracy of ± 10 per cent.

8. CONCLUSIONS

The following conclusions may be drawn from the results.

(1) The new concept of a sequence of hybrid inverse problems and a sequence of seismic response-drift constrained stiffness designs with respect to a ground stiffness parameter introduced here has provided a central backbone for developing a stiffness design method for a shear building supported by a prescribed pile–soil system. The sequence of seismic response-drift constrained stiffness designs can be found numerically by means of a sequential stepwise Taylor series expansion. An initial design for the sequence of seismic response-drift constrained stiffness designs can be derived without difficulty for a stiff ground by a method due to the senior authors, combining the hybrid inverse eigenmode formulation with the method regarding the lowest eigenvalue and lowest eigenmode as adjusting parameters.

(2) The sequence of seismic response-drift constrained stiffness designs could be non-monotonic with respect to a ground stiffness parameter resulting from the tuning of the fundamental natural period of a shear building with a fixed base with that of a shear beam ground. The present design method, which utilizes alternately the ground stiffness parameter and the building stiffness parameter in multiple design phases, can generate such a non-monotonic sequence. A seismic response-drift constrained stiffness design can be found by the present generator even in such a tuned region. Designing a building in such a region, however, should be avoided, as far as possible. A theoretical examination into such a case may be of some interest for laying the foundation of practical design regions.

(3) A set of sequences of seismic response-drift constrained stiffness designs for different levels of specified interstorey drifts (stiffness contour method) enables a designer to find a range of seismic response-drift constrained stiffness designs in which the scattering effect in the estimates of ground stiffnesses has been taken into consideration.

ACKNOWLEDGEMENTS

The present work was partially supported by Grant-in-Aid for Scientific Research, No. 05452251 and No. 07555644, from the Ministry of Education, Science and Culture of Japan. The financial support by Asahi Glass Foundation is also appreciated

APPENDIX I

Design earthquake

A set of ground motions compatible with a design velocity response spectrum $S_V(T;h)$ is defined here as the design moderate earthquake. $S_V(T;h)$ is defined at the bedrock level (see Figure 1) where T and h denote the natural period and damping ratio, respectively. A simplified version of the velocity response spectrum due to Newmark and Hall[20] is employed as $S_V(T;h)$. It is assumed here that the design displacement response spectrum $S_D(T;h)$ is related to $S_V(T;h)$ by $S_D(T;h) = (T/2\pi)S_V(T;h)$. $S_D(T;h)$ is now expressed as follows:

$$S_D^{(1)}(T;h) = \ddot{u}_{g\,\max}\{3{\cdot}32 - 0{\cdot}84\ln(100h)\}(T/2\pi)^2 \quad (T \leqslant T_L) \tag{23a}$$

$$S_D^{(2)}(T;h) = \dot{u}_{g\,\max}\{2{\cdot}36 - 0{\cdot}48\ln(100h)\}(T/2\pi) \quad (T_L \leqslant T \leqslant T_U) \tag{23b}$$

$$S_D^{(3)}(T;h) = u_{g\,\max}\{1{\cdot}86 - 0{\cdot}33\ln(100h)\} \quad (T_U \leqslant T) \tag{23c}$$

where $\ddot{u}_{g\,\max}$, $\dot{u}_{g\,\max}$, $u_{g\,\max}$ are the maximum acceleration, velocity and displacement, respectively, of the design earthquake defined at the bedrock and T_L, T_U are defined as

$$S_D^{(1)}(T_L;h) = S_D^{(2)}(T_L;h), \qquad S_D^{(2)}(T_U;h) = S_D^{(3)}(T_U;h) \tag{24a,b}$$

The amplitude of the design earthquake has been determined so that the mean value of the peak velocities of the free ground surface motions due to SHAKE program[19] would attain 25 cm/s. The model of soil layers is shown in Section 6. The amplitudes $\ddot{u}_{g\,\max}$, $\dot{u}_{g\,\max}$, $u_{g\,\max}$ are then 0·164 g, 20·0 cm/s and 15·0 cm, respectively.

Twenty artificial ground motions have been generated at the bedrock level through a revised version of SIMQKE program[21] so that the mean of those velocity response spectra for $h = 0{\cdot}02$ would coincide with the target velocity response spectrum. These artificial ground motions are utilized only at the stage of accuracy verification of the present design method (Section 7). The control points of the target spectrum are $(T(\mathrm{s}), S_V(\mathrm{cm/s})) = (0{\cdot}02, 0{\cdot}513), (0{\cdot}03, 0{\cdot}769), (0{\cdot}125, 8{\cdot}77), (0{\cdot}579, 40{\cdot}63), (3{\cdot}78, 40{,}63), (5{\cdot}00, 30{\cdot}75)$. In the range of shorter period the values proposed by Newmark and Hall[20] have been utilized. The envelope function is as follows:

$$\chi(t) = \begin{cases} 0{\cdot}164\,\mathrm{g}(t/3)^2 \quad (0 \leqslant t \leqslant 3\ \mathrm{s}) & (25\mathrm{a}) \\ 0{\cdot}164\,\mathrm{g} \quad (3 \leqslant t \leqslant 12{\cdot}5) & (25\mathrm{b}) \\ 0{\cdot}164\,\mathrm{g}\exp[-0{\cdot}24(t - 12{\cdot}5)] \quad (12{\cdot}5 \leqslant t \leqslant 25) & (25\mathrm{c}) \end{cases}$$

It is noted that the parameters in equation (23) have been modified from the original values so that the compatibility of the mean of velocity response spectra of the generated ground motions with $S_V(T;h)$ is improved in the high damping range, i.e. $h = 0{\cdot}10$.

APPENDIX II

Element stiffness matrix of interaction springs

$$
\begin{Bmatrix} f_1 \\ f_2 \\ f_3 \\ f_4 \\ f_5 \\ f_6 \end{Bmatrix} = k_{Ii}\, l_i
\begin{bmatrix}
\frac{13}{35} & \frac{11 l_i}{210} & -\frac{7}{20} & \frac{9}{70} & -\frac{13 l_i}{420} & -\frac{3}{20} \\
 & \frac{l_i^2}{105} & -\frac{l_i}{20} & \frac{13 l_i}{420} & -\frac{l_i^2}{140} & -\frac{l_i}{30} \\
 & & \frac{1}{3} & -\frac{3}{20} & \frac{l_i}{30} & \frac{1}{6} \\
 & & & \frac{13}{35} & -\frac{11 l_i}{210} & -\frac{7}{20} \\
 & \text{sym} & & & \frac{l_i^2}{105} & \frac{l_i}{20} \\
 & & & & & \frac{1}{3}
\end{bmatrix}
\begin{Bmatrix} v_{Pi} \\ \theta_{Pi} \\ v_{Si} \\ v_{P(i-1)} \\ \theta_{P(i-1)} \\ v_{S(i-1)} \end{Bmatrix}
\tag{26}
$$

where $f_1, \ldots, f_6$ denote the member-end forces corresponding to the member-end displacements $v_{Pi}, \theta_{Pi}, v_{Si}, v_{P(i-1)}, \theta_{P(i-1)}, v_{S(i-1)}$ (see Figure 1). This element stiffness matrix has been derived by assuming a cubic displacement function for a pile deflection and a linear displacement function for a shear beam ground.

APPENDIX III

Coefficients $a_{ij}, b_{ij}, c_{ij}, d_{ij}$, and sine and cosine spectra

$$
\begin{aligned}
a_{ij} &= \sqrt{h^{(i)} h^{(j)} \omega^{(i)} \omega^{(j)}}, & b_{ij} &= \omega^{(i)^2} + \omega^{(j)^2} + 2h^{(i)} h^{(j)} \omega^{(i)} \omega^{(j)} \\
c_{ij} &= h^{(i)} \omega^{(i)} + h^{(j)} \omega^{(j)}, & d_{ij} &= b_{ij}^2 - 4\omega_d^{(i)^2} \omega_d^{(j)^2}
\end{aligned}
\tag{27a–d}
$$

The sine spectrum $S^{(i)}$ and cosine spectrum $C^{(i)}$ are the mean values of $\max_t[S_i(t)]$, $\max_t[C_i(t)]$, respectively, where $S_i(t), C_i(t)$ are defined as follows.

$$
S_i(t) = -\frac{1}{\omega^{(i)}} \int_0^t \mathrm{e}^{-h^{(i)}\omega^{(i)}(t-\tau)} \{\sin \omega_d^{(i)}(t-\tau)\}\, \ddot{u}_g(\tau)\, \mathrm{d}\tau \tag{28}
$$

$$
C_i(t) = -\frac{1}{\omega^{(i)}} \int_0^t \mathrm{e}^{-h^{(i)}\omega^{(i)}(t-\tau)} \{\cos \omega_d^{(i)}(t-\tau)\}\, \ddot{u}_g(\tau)\, \mathrm{d}\tau \tag{29}
$$

REFERENCES

1. J. Penzien, C. F. Scheffey and R. A. Parmelee, 'Seismic analysis of bridges on long piles', *J. eng. mech. div. ASCE* **90(EM3)**, 223–254 (1964).
2. J. Penzien, 'Soil-pile foundation interaction', in R. L. Wiegel (ed.), *Earthquake Engineering*, Prentice-Hall, Chapter 14, Englewood Cliffs, NJ, 1970.
3. Y. Sugimura, 'Estimation of dynamic behaviours of soil layer–pile foundation interaction system', *Proc. anniversary symp. 50th Great Kanto Earthquake*, 133–140 (1973).
4. J. P. Wolf and G. A. Von Arx, 'Impedance function of group of vertical piles', *Proc. ASCE specialty conf. soil dyn. earthquake eng.* **2**, 1024–1041 (1978).
5. S. A. Anagnostopoulos, 'Pile foundation modelling for inelastic earthquake analyses of large structures', *Eng. struct.* **5**, 215–222 (1983).
6. G. Waas and H. G. Hartmann, 'Seismic analysis of pile foundations including soil-pile-soil interaction', *Proc. 8th world conf. earthquake eng.*, San Francisco **5**, 55–62 (1984).
7. Architectural Institute of Japan, *Proc. symp. dynamic soil–structure interaction* (1985) (in Japanese).

8. M. Kavvadas and G. Gazetas, 'Kinematic seismic response and bending of free-head piles in layered soil', *Geotechnique* **43(2)**, 207–222 (1993).
9. D. Badoni and N. Makris, 'Nonlinear response of single piles under lateral inertial and seismic loads, *Soil dyn. earthquake eng.* **15**, 29–43 (1996).
10. Tsuneyoshi Nakamura, I. Takewaki and Y. Shimano, 'Stiffness solution to a hybrid inverse seismic strain problem of a building frame–pile-soil system', *J. struct. constr. eng., Trans. Archi. Inst. Japan* **440**, 43–56 (1992) (in Japanese).
11. I. Takewaki and Tsuneyoshi Nakamura, 'Hybrid inverse mode problems for FEM–shear models', *J. eng. mech. ASCE* **121(8)**, 873–880 (1995).
12. Tsuneyoshi Nakamura and T. Yamane, 'Optimum design and earthquake-response constrained design of elastic shear buildings', *Earthquake eng. struct. dyn.* **14**, 797–815 (1986).
13. K. Hirayama, 'Stiffness design for specified seismic member strains of a plane building frame supported by a two-dimensional finite-element ground–pile system', *Thesis for Master of Eng.*, supervised by Tsuneyoshi Nakamura and I. Takewaki, Kyoto Univ., 1996 (in Japanese).
14. Tsuneyoshi Nakamura and Yutaka Nakamura, 'Stiffness design of 3-D shear buildings for specified seismic drifts, *J. struct. eng. ASCE* **119(1)**, 50–68 (1993)
15. J. N. Yang, S. Sarkani and F. X. Long, 'A response spectrum approach for seismic analysis of nonclassically damped structures', *Eng. struct.* **12**, 173–184 (1990).
16. Tsuneyoshi Nakamura and M. Ohsaki, 'Sequential optimal truss generator for frequency ranges', *Comput. methods appl. mech. eng.* **67**, 189–209 (1988).
17. Tsuneyoshi Nakamura and M. Ohsaki, 'Sequential generator of earthquake-response constrained trusses for design strain ranges', *Comput. struct.* **33**, 1403–1416 (1989).
18. A. Shibata, *Structural Analysis of Seismic-resistant Structures*, Morikita Corp. (1981) p. 87 (in Japanese).
19. P. B. Schnabel, J. Lysmer and H. B. Seed, 'SHAKE: A computer program for earthquake response analysis of horizontally layered sites', A computer program distributed by NISEE/Computer Applications, Berkeley, 1972.
20. N. M. Newmark and W. J. Hall, *Earthquake Spectra and Design*, Earthquake Eng. Research Institute, Berkeley, 1982.
21. D. A. Gasparini and E. H. Vanmarcke, 'Simulated earthquake motions compatible with prescribed response spectra -SIMQKE', A computer program distributed by NISEE/Computer Applications, Berkeley, 1976.